Colonic hypersensitivity and low-grade inflammation in a spontaneous animal model for functional gastrointestinal disorders

Mathieu Meleine, Alison Accarie, Lucas Wauters, Joran Toth, Guillaume Gourcerol, Jan Tack, Ricard Farré, Tim Vanuytsel

Colonic hypersensitivity and low-grade inflammation in a spontaneous animal model for functional gastrointestinal disorders.

Mathieu Meleine[1,2,*], Alison Accarie[1,*], Lucas Wauters[1], Joran Toth[1], Guillaume Gourcerol[2], Jan Tack[1], Ricard Farré[1], Tim Vanuytsel[1].

[1]: Translational Research Center for Gastrointestinal Disorders (TARGID), University of Leuven, Leuven, Belgium.

[2]: Inserm UMR 1073, Institute for Innovation and Biomedical Research, Rouen University, Rouen, France.

* Contributed equally to the study.

Abstract

Background: A complex interplay between a failing intestinal barrier and low-grade inflammation leading to sensorimotor disturbances is an often-cited mechanism in the pathogenesis of functional gastro-intestinal disorders (FGID). However, the cause-consequence relationship between these features has not been clearly established. We previously described jejunal alterations in the normoglycemic BB-rat (BBDP-N) model proposing this model as a suitable animal model to study FGID pathophysiology. The current study explores colonic permeability, inflammation and sensitivity of the BB-rat.

Methods: Colonic tissue of BBDP-N and control (BBDR) rats at 50, 90, 110, 160 and 220 days ($n \geq 7$ per group) was used to assess intestinal permeability in Ussing chambers and inflammation, including infiltration by eosinophils, mast cells and eosinophil peroxidase (EPO) activity. Anxiety-like symptoms were evaluated at 50, 90 and 220 days and colonic sensitivity at 160 and 220 days by measuring the visceromotor response (VMR) to isobaric colo-rectal distensions.

Keys results: Lamina propria eosinophils and mast cells infiltration and increased EPO activity were demonstrated from 90 days onwards. Increased permeability and myenteric ganglionitis was observed in the oldest BBDP-N rats. At 220 days, the VMR was significantly increased suggesting colonic hypersensitivity. At the same age increased anxiety-like behavior was observed.

Conclusion and inferences: We demonstrated a lamina propria eosinophil and mast cell infiltration preceding visceral hypersensitivity in the colon of the BBDP-N rat, reminiscent of patients with FGID. These findings help elucidating pathogenetic pathways in FGID and further validate the BBDP-N rat as an attractive model to study pathophysiology and therapy of FGID.

Keywords: BioBreeding rat, Functional gastrointestinal disorder, intestinal permeability, visceral hypersensitivity

Abbreviations:

BBDP-N: Diabetes-prone BiobBreeding rat

BBDR: Diabetes-resistant BiobBreeding rat

C2R: Chromotrope 2R

FD: Functional dyspepsia

EPO: Eosinophil peroxidase

FGID: Functional gastrointestinal disorders

FITC-Dx4: 4kDa dextrans conjugated to fluorescein isothiocyanate

MCPT2: Mast cells protease 2

MPO: Myeloperoxidase

PMN: Polymorphonuclear cells

TEER: Transepithelial electrical resistance

VMR: Visceromotor response

Keys points:

- The interplay between permeability, inflammation and sensitivity is proposed as a key component in the pathophysiology of functional gastrointestinal disorders (FGID) but their interaction is not fully understood yet. We characterized the colonic features of the BBDP-N, a spontaneous model of FGID.
- We found a positive association between lamina propria permeability and mast cells and eosinophils density in old rats, associated with a colonic hypersensitivity and anxiety-like symptoms. However, no direct link could be established between permeability or inflammation and sensitivity, suggesting a different pathophysiology.
- Our results further validate the BBDP-N as a model to further explore pathophysiology and treatment options for FGID.

1. Introduction

Symptoms in functional gastrointestinal disorders (FGIDs) like irritable bowel syndrome (IBS) result from a complex interplay of impaired gastrointestinal functions in the absence of any obvious organic, structural or metabolic cause (1, 2). As a consequence, the pathogenesis of these heterogeneous disorders is still poorly understood and the therapeutic management remains challenging. A failing intestinal barrier in combination with low-grade inflammatory processes affecting both the enteric and extrinsic nervous system function are frequently cited mechanisms to explain sensorimotor abnormalities and subsequent symptoms in IBS patients (3-7). However, although mucosal immune activation and a barrier defect have also been shown in at least a subset of IBS patients (3, 4), their interaction is not completely understood. Moreover, it is clearly established that inflammation *per se* can modulate intestinal permeability (8-12), indicating that the impaired barrier function may also be a secondary phenomenon. Understanding the precise sequence of the barrier defect, immune activation and visceral hypersensitivity in a pathophysiological context would be of great interest in order to improve diagnosis and propose relevant therapeutic strategies. For that purpose, a spontaneous animal model sharing the relevant GI features related to FGIDs would be instrumental to unravel this complex sequence of events in patients. BioBreeding (BB) rats are derived from an outbred Wistar rat colony and have been extensively studied as a model of type 1 diabetes (13- 15). It consists of a diabetic-resistant (BBDR) strain, used as control, and a diabetic-prone (BBDP) strain. Depending on the environmental and dietary conditions, 50 to 90% of BBDP rats between 60 and 120 days old will develop diabetes characterized by marked glycosuria, hyperglycemia, hyperketonemia and ketonuria (16-18). At the gastrointestinal level, diabetic animals show evidence of increased intestinal permeability, prior to onset of diabetes (19, 20), combined with transmural intestinal inflammation and loss of nitrergic motor neuron function which results in disordered motility. Previous work from our group demonstrated an early jejunal hyperpermeabililty in normoglycemic BB-rats (BBDP-N) preceding a polymorphonuclear (PMN) granulocyte infiltration, including mast cells and eosinophils, starting in the lamina propria and progressively expanding to the jejunal neuromuscular layers in a subset of rats (5, 21). Together, these data suggest a disease-initiating role for intestinal permeability in the gastrointestinal impairments observed in the BBDP-N that finally lead to motor dysfunction. However, this previous study focused on the small intestinal features and although these alterations are also present in the proximal small intestine of IBS patients (3-4), most human studies have focused on the colon and symptoms are thought to originate mostly from the lower GI tract. Moreover, data on visceral sensitivity are entirely lacking in this model as well as on associated co morbidities such as anxiety and depression which are frequently described in FGID patients with chronic discomfort and pain.

Therefore, we aimed to characterize colonic permeability, inflammation, sensitivity and anxiety-like symptoms of the BBDP-N rat over time. Together with previous studies this work will advance our understanding of the gastrointestinal dysfunction occurring in this model.

2. Material and Methods

2.1 Animals

Breeding pairs of BBDR and BBDP-N rats were obtained from the Ottawa Hospital Research Institute (Dr. Fraser Scott; Ottawa, ON, Canada) and further bred in the conventional animal facility of the KU Leuven, Belgium. Rats were housed in wire-meshed cages on a 12-hours light/dark cycle and had *ad libitum* access to drinking water and standard rat chow. Glycemia was measured on tail blood on a weekly basis using a OneTouch®Verio® glucometer (LifeScan, Diegem, Belgium) starting from 70 days of age. Diabetes onset was characterized by glycemia values above or equal to 250 mg dL^{-1} on two consecutive occasions (21). Since the purpose of the current study focused on gastrointestinal features unrelated with hyperglycemia, only BBDR and normoglycemic BBDP (BBDP-N) rats were included. In the current cohort of rats 70% of rats developed diabetes by the age of 160 days. All animal experiments were approved by the ethics committee for animal experiments of the University of Leuven.

2.2 Experimental design

BBDR and BBDP-N rats of 50, 90, 160 and 220 days old were euthanized by cervical dislocation and exsanguination ($n \geq 7$ per group). These time points were selected based on previous work reporting altered intestinal permeability in BBDP-N rats starting from 50 days, prior to the onset of diabetes (21), followed by a progressive transmural immune cell infiltration at later time points (90, 160 and 220 days). After euthanasia, blood was collected in a 10mL BD Vacutainer® tube containing 18mg EDTA (BD, Plymouth, UK), colon was harvested and stored in ice-cold Krebs-Ringer buffer (2.5 mM $CaCl_2$, 5.9 mM KCl, 1.2 mM $MgCl_2$, 120.9 mM NaCl, 14.4 mM $NaHCO_3$, 1.2 mM NaH_2PO_4, and 11.5 mM glucose; all purchased from Merck, Overijse, Belgium), continuously gassed with carbogen (95%O2, 5%CO2) until further processing. At least 2 days before sacrifice, visceral sensitivity was assessed in the oldest rats (160 and 220 days old) as described below.

2.3 Assessment of epithelial barrier function

Four segments of distal colon of each animal were mounted in modified Ussing chambers (Mussler Scientific Instruments, Aachen, Germany) after removal of the seromuscular layer, with an exposed area of 0.096 cm^2. The luminal and basolateral compartments were filled with Krebs-Ringer bicarbonate buffer, supplemented with 10 mM glucose. Solutions were kept at 37°C and gassed with carbogen. Transmucosal potential difference was continuously monitored using Ag/AgCl electrodes. The transepithelial electrical resistance (TEER) was calculated according to Ohm's law from the voltage deflections induced by bipolar current pulses of 50 µA every 60 s with a duration of 200 ms. The TEER values were registered for each tissue at 30 min intervals. The average TEER between 90 and 120

minutes was calculated over the four tissues per animal. These time points were selected because a stable TEER plateau was reached in most of the tissues between 90 and 120 minutes after mounting. Molecular flux was studied by adding 4 kDa dextrans conjugated to fluorescein isothiocyanate (FITC-Dx4, final concentration 1 mg mL^{-1}, Sigma-Aldrich, Diegem, Belgium) to the luminal compartment after a 40-minute stabilization period in tissues of animals of 50, 90, 110, 160 and 220 days. Fluorescence was determined in samples from the basolateral side, taken with 30 min intervals during 120 minutes. The fluorescence values were converted to pmol cm^{-2} based on a standard curve included for each analysis. Average cumulative passage of FITC-Dx4 between 90 and 120 minutes after adding the probe was calculated for each animal.

2.4 Eosinophil peroxidase and myeloperoxidase activity

The eosinophil peroxidase (EPO) and myeloperoxidase (MPO) activity was determined in colonic mucosa + submucosa by a spectrophotometric assay, based on the conversion of o-Phenylenediamine (OPD) to its colored oxidized form in the presence of H_2O_2. Briefly, the mucosa and submucosa were separated from the seromuscular layers by gentle dissection and immediately snap-frozen in liquid nitrogen. Extraction of EPO and MPO was performed by homogenization of the tissue in a 0.5% hexadecyltrimethylammonium chloride (Sigma-Aldrich, Diegem, Belgium) buffer at pH 6.0 followed by two freeze-thaw cycles and a centrifugation step (14000g, 30min, 4°C). For the EPO, reaction mix containing OPD (3mM), Potassium Bromide (6mM) and H_2O_2 (8.8mM) in HEPES buffer (50mM) at pH 6.5 was added to supernatant. For the MPO, reaction mix containing TMB (400µM), resorcinol (120µM) and (2.2mM) in phosphate citrate buffer at pH 5 was added to the supernatant (22). After 1 minute, the reaction was stopped with H_2SO_4 (4M) and absorbance was read at 492 nm. Human EPO or MPO (Sigma-Aldrich, Diegem, Belgium) was used as a standard. Data are expressed in µg/g tissue.

2.5 Real-time PCR

After separation of the mucosa and submucosa from the underlying layers by gentle dissection, the tissue was homogenized in TRIzol reagent (Invitrogen, Ghent, Belgium) and stored at −80°C until further processing. Total RNA was extracted and further purified using a High Pure RNA isolation kit (Roche Diagnostics, Vilvoorde, Belgium) according to the manufacturer's instructions. c-DNA was synthesized from 2 µg RNA using the qScript cDNA Supermix kit (Quanta Biosciences, Gaithersburg, MD, USA). The real-time PCR reaction was performed on a LightCycler 480 system with SYBR Green I Master mix (Roche Diagnostics, Vilvoorde, Belgium). Specific primers for sensitivity-, permeability- and inflammation-related genes were designed using NCBI Primer-Blast (Supplementary table 1). A three-step amplification program was used: 95°C for 10 min followed by 45 cycles of amplification (95°C for 10 s, 60°C for 15 s, 72°C for 10 s) and finally a melting curve program. Target mRNA expression was quantified relative to the housekeeping gene Hprt1 using the $-2\Delta\Delta Ct$ method.

2.6 Histology

A 1-cm section of distal colon was fixed overnight in paraformaldehyde 3.7% (Sigma-Aldrich, Diegem, Belgium) and embedded in paraffin. Sections of 5 µm were cut using a microtome and stained with hematoxylin and eosin (H&E). Similar to our previous study in the small intestine, polymorphonuclear (PMN) granulocytes were counted in the *lamina propria* in 5 non-overlapping high-power fields and in 50 ganglia of the myenteric plexus in a blinded fashion (21). A ganglion was defined as a collection of at least two adjacent neuronal cell bodies.

Specific quantification of eosinophils was performed using Chromotrope 2R staining. Briefly, following deparaffinization with xylene and rehydration with serial ethanol dilutions, slides were immersed for 1 hour in a solution containing Phenol (106.2 mM; Sigma-Aldrich, Diegem, Belgium) and Chromotrope 2R (21.3 mM; Sigma-Aldrich, Diegem, Belgium). A counterstaining was performed by the application of hematoxylin during 15s on the sections. The number of positive cells was counted in 3 non-overlapping high-power fields per slide in a blinded manner and expressed as the number of chromotrope 2R positive cells per area of lamina propria.

2.7 Immunohistochemistry

After deparaffinization and rehydration, endogenous peroxidase activity was inhibited with 5% H_20_2 for 30 minutes and non-specific binding sites were blocked with Protein Blocking solution (Dako, Glostrup, Denmark). Slides were incubated overnight with anti-mast cell protease 2 (MCPT2) antibody (1:500; Moredun Scientific, Penicuik, Scotland, UK) at 4°C then 1 hour at room temperature with a horse anti-mouse biotinylated secondary antibody (1:200; Vector Laboratories, Burlingame, CA, USA). Finally, slides were incubated with 3,3'-diaminobenzidine (DAB substrate development kit, Vector laboratories) for 3 minutes. The number of MCPT-2 positive cells was counted in 3 non-overlapping high-power fields per slide in a blinded manner and expressed as the number of MCPT2-positive cells per area of lamina propria.

2.8 Colonic sensitivity

Colonic sensitivity was assessed by recording abdominal muscle activity in response to isobaric colorectal distensions. Under Isoflurane (Iso-Vet, Piramal Healthcare, Northumberland, UK) anesthesia (2.5% in 3L min^{-1} air), a 2-cm incision was performed in the abdominal skin. A Physiotel ETA-F10 telemetric transmitter (Data Sciences International, MC s'Hertogenbosch, The Netherlands) was inserted subcutaneously towards the flank of the animal and secured in place with 6-0 sutures (Ethicon, Somerville, NJ, United States). The non-insulated tips of the electrodes, connected to the transmitter, were tunnelled into the left and? right external abdominal oblique muscle with an 18G needle (Terumo Europe, Leuven, Belgium) and maintained in parallel (±5 mm apart) using 6-0 sutures

(Ethicon, Somerville, NJ, United States). Following surgery, rats were left undisturbed for at least 8 days before the colorectal sensitivity experiments.

On the day of the measurement, rats were lightly anesthetized with Isoflurane to allow smooth insertion of the distension probe into the colon with the distal end of the balloon at 1.5cm from the anal margin. The balloon was self-made with a polyethylene bag attached to the tip of a polyethylene tubing (1.67mm inner diameter; 2.42mm outer diameter, Becton Dickinson and Cie, Franklin lakes, NJ, United states). The length of the non-inflated balloon was 4 cm. After balloon insertion rats were placed in a makrolon type II cage and allowed to recover from anesthesia for at least 20 minutes. Consciousness of the rats was assessed by both the oculopalpebral reflex and response to tail pinch. Graded isobaric colorectal distensions increasing from 15 to 60mmHg were applied using a Barostat Distender series IIR (G&J Electronics, ON, Canada) with 15mmHg increment steps, a duration of 20s for each step and 4-min intervals between distensions.

The visceromotor response (VMR) was measured and quantified using DataQuest software (Data Sciences International, MC ‘sHertogenbosch, The Netherlands). For analysis, the mean value of the resting EMG signal 20 s prior to distension (i.e., basal activity) was subtracted from the mean value of the electromyography signal evoked during the 20 s distension. To account for the different balloon and colonic diameters, the data were expressed as the linear regression of the VMR in response to wall tension stimulation calculated according to Laplace’s law applied to a cylindrical vessel:

$$T = P * r$$

where P (mmHg) is the pressure applied and r (m) the radius of the vessel (i.e. the intra-colonic balloon). To calculate the radius, we used the following formula with the assumption of an ellipsoid shape:

$$r=\sqrt{(V/(4/3\pi)*R)}$$

where V (L) is the intra-colonic balloon volume and R (m) the half great axis of the ellipsoid.

The volume of the intracolonic balloon is measured by the Barostat device and determined with the software Protocole Plus Delux version 6.7R.

2.9 Behavioral assessment

In a separate batch of rats (n=7 per group), anxiety-like symptoms were assessed with two different behavioral tests on two separate days by the same investigator (AA). Experiments were done under 40 lux lighting. *Marble Burying-behavior:* 20 marbles (1 cm diameter) were placed in a regular rat cage (26x42x18 cm) on 5cm of bedding. Rats were followed during 20 min and the number of buried objects were counted. A higher number of buried marbles signifies a more anxious state (23). *Open field test:*

rats were placed in a grey open field (73x73cm divided in 25 squares) in which an inner zone of 12 squares was defined. Rats were recorded for 5 min. The number of squares crossed was used to evaluate the locomotor activity and the time spent in the inner zone and the number of entries as anxiety-like behavior (24-25).

2.10 Statistical analysis

Mann-Whitney or a Friedman test were used comparing groups at each time point. Data are presented as mean ± standard error of the mean (SEM). For colonic sensitivity experiments, an F-test was used to compare slopes and elevations of linear regression curves modelling visceromotor response to wall tension. The correlations were tested with the Spearman test, all values from all age group of BBDR and BBDP-N were separately analyzed. Data were analyzed using Prism 5.01 (GraphPad Software, San Diego, CA, USA).

3. Results

3.1 Impaired colonic barrier function

Colonic barrier function was assessed in rats of 50, 90, 110, 160 and 220 days. No evidence of altered colonic permeability was observed in BBDP-N rats at early ages (50, 90 and 110 days). At 160 days, the TEER was significantly lower in BBDP-N rats compared to controls (Fig1A). Concomitantly, the paracellular passage of FITC-Dx4 started to increase in the BBDP-N animals at 160 days (Fig 1B). At 220 days, a drop in TEER values was observed in control rats with similar values in BBDP-N rats (Fig 1A). Similarly, the paracellular passage of FITC-Dx4 was higher in control rats at day 220. However, at this age, the paracellular passage of FITC-Dx4 was still significantly higher in BBDP-N rats (Fig 1B). These data combined suggest an increased paracellular permeability in the older BBDP-N rats.

In order to unravel the molecular alterations underlying this increased permeability, mRNA expression of intestinal tight junction proteins claudin 1 (CLDN1), CLDN2, Zona Occludens 1(ZO-1) and Occludin (Occl) were measured in colonic lamina propria of old rats (160 and 220 days). However, no difference was found between BBDR and BBDP-N rats at either age (Suppl. Fig 1).

3.2 Mucosal and neuromuscular inflammation

An infiltration of PMN (Fig 2A and 2C) was observed in the lamina propria starting from 110 days, which paralleled the increased number of eosinophils (Fig 3A and 3C) and EPO activity measured in the tissue (Fig 3B) while the MPO activity was only increased at 220 days (Fig2B).

At the same time, an infiltration of PMN was found in the myenteric ganglia of some rats which progressed with ageing (2/6 at 110 days, 6/8 at 160d and 7/9 at 220d) while this was virtually absent in the control strain (Fig 2D, 2E). No infiltration of PMN or eosinophils was found in the youngest rats (50 and 90 days) while the mast cell density already started to increase significantly from 90 days onwards (Fig 4A). Only a transient increase in IL-4, IL-13 and IL-1β was observed at 160 days of age (Table 1).

3.3 Colonic hypersensitivity in old BBDP-N rats

As colonic permeability and low-grade inflammation are often linked with an altered colonic sensitivity in IBS patients and animal models, we assessed colonic sensitivity in the oldest rats, i.e. at 160 and 220 days. Colorectal sensitivity was assessed by VMR to wall tension induced by isobaric distensions. While the slope and intercept of the linear regression curves were comparable between BBDR and BBDP-N rats at 160 days (Fig 5A), a significant upward shift of the curve was observed in 220 days old BBDP-N rats compared to controls (F ratio=39,2501, DFn=1, DFd= 57; $p<0.0001$, Fig 5C)) indicating colonic hypersensitivity. Moreover, a reduction in colonic compliance, assessed by the ratio of the intra-colonic balloon volume corresponding to the pre-established distension pressures, was observed at

both ages in the BBDP-N strain (Fig 5B and D). The lower compliance resulted in lower wall tension exerted for a given pressure in BBDP-N animals and might reflect an impaired colonic wall tone.

3.4 Anxiety-like symptoms

Anxiety-like symptoms were evaluated with two different tests. With the open field test, no differences were found for the number of squares crossed over the 5 minutes of recording suggesting an equivalent mobility in the different strains (Fig 6A). Also, no difference was observed in the time spent in the inner zone at either age (Fig 6C) nor in the number of entries (Fig 6B), suggesting similar anxiety levels. However, with the marble burying test, while no differences were visible in young rats of 50 and 90 days, significantly more objects were buried by the oldest BBDP-N compared to control rats (Fig 6A-B) suggesting a more pronounced anxiety-like behavior compared to controls.

3.5 Associations between permeability, inflammation and sensitivity.

A positive correlation was found in BBDP-N (all age groups combined) only between the PMN cell density in the colonic lamina propria and the passage of the FITC-dextran 4kDa (r^2=0.74 p=0.0004 Figure 7A). Similarly, lamina propria density of eosinophils and mast cells in the colonic lamina propria also correlated positively with the passage of FITC-dextran 4kDa (r^2=0.68 p=0.0017 Figure 7B and r^2=0.38 p=0.02 Figure 7C respectively). However, no correlations were observed between the VMR and measures of inflammation or permeability for the two oldest group of rats (Suppl. Fig. 2).

4. Discussion

Our study aimed to characterize colonic features of the BBDP-N, a spontaneous animal model sharing key small intestinal characteristics with human FGID (21). In this model, we observed an early inflammatory reaction from 90-110 days onwards, mainly driven by mast cells and eosinophils which preceded an impaired barrier function coinciding with colonic hypersensitivity and anxiety-like behavior in the oldest age group (220 days). Our findings suggest that, in the colon, permeability is not the driver of the immune activation and may rather be a consequence of inflammation.

The pathophysiology of FGIDs is still poorly understood. A variety of GI symptoms related to altered motility and/or visceral hypersensitivity are supported by multiple pathophysiological mechanisms but their intricate connection and relevance in the disease process are still a matter of debate. Previous work in functional dyspepsia and IBS highlighted a strong association between altered tight junctions and lamina propria permeability that may facilitate access of luminal antigens into the sub-epithelial layers of the gut wall, causing immune activation and visceral hypersensitivity (26, 27). However, the cause-consequence relationship of these alterations is still unclear since no longitudinal studies are available in human FGID and anti-inflammatory or barrier-enhancing treatment approaches have not been very successful to date.

The pathophysiological features of the BB-rat model were previously described in detail for the jejunum where an increased permeability in young BBDP-N rats, associated with impaired expression of tight junction related proteins, was observed prior to infiltration of mast cells, eosinophils (5, 21). However, this paradigm was not confirmed at the colonic level in the current study, revealing regional differences within the GI tract of the BB-rat model. A few studies reported on other colonic alterations in the BBDP strain with a decrease in circular muscle β-adrenoreceptor expression in old hyperglycemic rats, indirectly suggesting motility dysfunction (28). In BBDP-N rats, an increased incidence of megacolon associated with inflammatory infiltrate and destruction of autonomic ganglia and muscularis propria was previously reported (29). Nevertheless, no study offered a complete overview of the colonic features of the BBDP-N rat.

In the colon, the first pathological feature we observed was a mast cell infiltration in the *lamina propria* of 90-day old BBDP-N rats which preceded colonization by PMN including eosinophils. The latter were also found in the neuromuscular layers as shown by a clear infiltration into the myenteric ganglia which progressed over time. Interestingly, although there was no change in eosinophil number in younger rats (D50 and D90), the EPO activity was already slightly higher, suggesting that resident eosinophils are already more active in young BBDP-N than in BBDR rats and might participate to the recruitment of other immunes cells (30). Mast cells and eosinophils are known to secrete soluble factors known to alter epithelial permeability (31-33) through destabilization of tight junctions (10, 11). Despite the

obvious involvement of eosinophils and mast cells in the colonic inflammation of the BBDP-N rat, we cannot rule out the role of other inflammatory cells such as previously described in FGIDs (34). MPO activity, reflecting mainly neutrophil, monocyte and macrophage activation (35), was only increased at the later time point (D220) suggesting that the activation of those cell types is not involved in the early inflammatory phase but may have a role in its maintenance. This observation is consistent with the upregulation of colonic iNOS, mainly expressed by macrophages, seen at 220 days and which was previously found in the jejunum (21).

The second feature altered in BBDP-N rats is colonic permeability as shown by decreased TEER and increased FITC-Dextran 4kDa passage in old rats. Intestinal permeability is the result of both transcellular and paracellular pathways. The paracellular route comprises (i) the pore pathway: a large-capacity pathway for small solutes and (ii) the leak pathway: a small-capacity pathway for larger molecules. TEER gives a picture of pore and leak pathways while the flux of macromolecules like dextrans is regulated by the leak pathway only (35, 36). Our results suggest that both pathways are altered in BBDP-N animals but only transiently for the TEER (D160) since the difference was lost in 220 days old rats while the leak pathway is significantly upregulated. Previous preclinical and clinical reports highlighted an increasing colonic permeability with age, using passage of macromolecules as a mucosal-to-serosal flux indicator (37, 38) that could explain why the difference in TEER between groups subsided in older rats.

At the molecular level, barrier function is regulated principally by the tight junctions of the apical complex consisting of a set of transmembrane proteins (claudins and occludin) and scaffolding proteins (ZO-1) that attach transmembrane protein to the cytoskeleton (39). In our study, no difference in tight junction mRNA expression was found between BBDP-N and BBDR groups which is particularly intriguing regarding the alteration of the paracellular pathway at D160 in BBDP-N rats. To explain such a discrepancy, we can speculate that, rather than a change in expression, hyperpermeability is due to a remodelling of tight junction at protein level or altered phosphorylation state as it was previously demonstrated (40, 41).

We previously demonstrated that permeability and immune activation in the jejunum occurred at an earlier age compared to the colon (21), potentially identifying small intestinal permeability as the driver behind local and subsequently more generalized GI inflammation. This hypothesis has been demonstrated in the IL10 knockout model for colitis where normalization of small intestinal permeability attenuated colonic inflammation (41).

In the present study, we demonstrated a positive correlation between the immune cell density in the colonic lamina propria (PMN, eosinophils and mast cells) and the transmucosal passage of 4kDa fluorescein isothiocyanate (FITC) dextran suggesting an important role of these cells. Previous pre-

clinical and clinical studies including some from our group already demonstrated that mast cell seems to be directly related to the intestinal permeability (33, 42). Further experiments in which rats are treated with a mast cell stabilizer or anti-inflammatory drugs will be necessary to confirm our hypothesis of a direct link between intestinal permeability and mast cells and to further strengthen our model.

We pointed out a colonic hypersensitivity in 220 days old BBDP-N rats. This feature is of particular interest since, together with the Wistar-Kyoto strain and the Flinders Sensitive Line strain, this is a rare spontaneous model of colonic hypersensitivity in rats (43, 44). According to our data, colonic hypersensitivity in the BBDP-N rats does not seem to be directly related to increased permeability or inflammation since no association could be demonstrated. Further studies are warranted to describe more specifically pathophysiological mechanisms at the source of colonic hypersensitivity.

As described in patients, immune activation, increased permeability and hypersensitivity are often linked with symptoms of anxiety and depression. In our model, we assessed anxiety-like symptoms in the same rats at 50, 90 and 220 days with two well-established tests, the open field and the marble burying test. With the open field test, no differences were found although it seems that young rats display more anxiety-like symptoms than older rats, but this needs to be confirmed since we lost several animals in this longitudinal evaluation due to the development of hyperglycemia. With the marble burying test, an anxiety-like behavior was demonstrated in old rats which already became apparent at 90 days. While the two tests are supposed to measure the same parameter, disparate results were also found by other studies (45). Our results suggest that the marble burying might be more sensitive than the open field to detect small changes in the anxiety level. Pain-related anxiety symptoms become notable and measurable in case of chronic pain. It might be that, in our study, we are only at the beginning of the anxiety-symptoms and further, more prolonged studies are needed to investigate what is happening when the colonic hypersensitivity can be considered as chronic. Furthermore, it has been pointed out that those two tests are involving different neurochemical brain circuits (46). These results add important strength to the model as there only few spontaneous animal models which are showing both pain and anxiety-like behaviour in the context of hyperpermeability and immune activation. Taken together, our results on the BB-rat model bring new opportunities to further unravel the mechanisms behind the effect of triggers such as stress on the onset of symptoms and their severity. Moreover, to definitely answer the cause-consequence relationship between permeability, immune activation, hypersensitivity and anxiety, treatment studies investigating the effect of normalizing permeability or inflammation are needed and subject of ongoing research. In the last couple of years, alterations in the microbiota composition have been shown to be related to FGID, to contribute to the intestinal permeability, low grade inflammation and visceral hypersensitivity (47, 48). The potential role of the microbiota in the BioBreeding rat has been investigated in several studies.

However, they mainly focused on the effect of dysbiosis on the onset of the diabetes (49, 50). Brugman *et al.* demonstrated a specific early increase of *Bacteroides* in the BBDP rats that will develop diabetes later in their life compared to those that will not develop diabetes (49). Unfortunately, this study did not include the control group (BBDR). Also, no studies have focused on the normoglycemic BBDP animals and the relation to the described enteropathy. Studies investigating contributing luminal factors causing the intestinal pathology, including microbiota and nutrients, are currently ongoing.

To conclude, our findings confirming immune activation, impaired colonic barrier function, visceral hypersensitivity, anxiety-like symptoms with a very clear time frame which further validate the BBDP-N rat as an insightful model to unravel the pathophysiology of human FGIDs. These features are also of particular interest in the pre-clinical assessment of the efficacy of novel barrier-enhancing, anti-inflammatory or analgesic therapies for this group of disorders that remain extremely frequent and difficult to treat.

Acknowledgements, Funding, and Disclosures

Funding was provided by a Methusalem grant from Leuven University to JT and a starting grant from Leuven University to TV. LW and TV are supported by the Flanders research foundation (FWO Vlaanderen) through a doctoral fellowship and senior clinical research mandate respectively. The authors also acknowledge Prof. Guy Boeckxstaens to provide us with the hard- and software to record the visceromotor response.

The authors disclose no conflicts of interest.

Authors contribution

MM: study design, data acquisition; analysis and interpretation of data; drafting of the manuscript; critical revision of the manuscript.

AA study design, data acquisition; analysis and interpretation of data; drafting of the manuscript; critical revision of the manuscript.

LW analysis and interpretation of data; critical revision of the manuscript.

JT data acquisition

GG critical revision of the manuscript; funding.

RF analysis and interpretation of data; critical revision of the manuscript.

JT critical revision of the manuscript; funding.

TV study design; analysis and interpretation of data; drafting of the manuscript; critical revision of the manuscript; funding.

References

1. Tack J, Talley NJ, Camilleri M, Holtmann G, Hu P, et al. (2006) Functional gastroduodenal disorders. *Gastroenterology* 2006;130: 1466–1479
2. Longstreth GF, Thompson WG, Chey WD, Houghton LA, Mearin F, et al. (2006) Functional Bowel Disorders. *Gastroenterology* 2006;130: 1480–1491
3. Matricon J, Meleine M, Gelot A, Piche T, Dapoigny M, et al. Review article: Associations between immune activation, intestinal permeability and the irritable bowel syndrome. *Aliment Pharmacol Ther* 2012;36: 1009–1031
4. Martinez C, Lobo B, Pigrau M, Ramos L, Gonzales-Castro AM, et al. (2013) Diarrhoea-predominant irritable bowel syndrome: an organic disorder with structural abnormalities in the jejunal epithelial barrier. *Gut* 2013;62:1160-1168
5. Vanuytsel T, Di Giovangiulio M, Vanormelingen C et al. The Normoglycemic BB-DP Rat As a Model for Functional Gastrointestinal Disorders: The Implication of Mast Cells and Eosinophils *Gastroenterology*. 2015;148:S-778
6. O'Malley D. Immunomodulation of enteric neural function in irritable bowel syndrome. *World J Gastroenterol*. 2015;21:7362-7366.
7. Tornblom H, Lindberg G, Nyberg B, Veress B (2002) Full-thickness biopsy of the jejunum reveals inflammation and enteric neuropathy in irritable bowel syndrome. *Gastroenterology* 2002;123: 1972–1979
8. Wyatt J, Vogelsang H, Hubl W, Waldhoer T, Lochs H Intestinal permeability and the prediction of relapse in Crohn's disease. *Lancet* 1993;341: 1437–1439.
9. Hollander D, Vadheim CM, Brettholz E, Petersen GM, Delahunty T, et al. Increased intestinal permeability in patients with Crohn's disease and their relatives. A possible etiologic factor. *Ann Intern Med* 1986;105: 883–885
10. Capaldo CT, Nusrat A Cytokine regulation of tight junctions. *Biochim Biophys Acta* 2009;1788: 864–871
11. Odenwald MA, Turner JR Intestinal Permeability Defects: Is It Time to Treat? *Clin Gastroenterol Hepatol* 2013;11:1075-1083
12. Suzuki T Regulation of intestinal epithelial permeability by tight junctions. *Cell Mol Life Sci* 2013;70: 631–659
13. Like AA, Butler L, Williams RM, Appel MC, Weringer EJ, Rossini AA. Spontaneous autoimmune diabetes mellitus in the BB rat. *Diabetes* 1982;31(Suppl 1 Pt 2):7-13.
14. Rossini AA, Handler ES, Mordes JP, Greiner DL Human autoimmune diabetes mellitus: lessons from BB rats and NOD mice—Caveat emptor. *Clin Immunol Immunopathol* 1995;74: 2–9

15. Like AA, Rossini AA, Guberski DL, Appel MC, Williams RM Spontaneous diabetes mellitus: reversal and prevention in the BB/W rat with antiserum to rat lymphocytes. *Science* 1979 206: 1421–1423
16. Visser JT, Lammers K, Hoogendijk A, Boer MW, Brugman S, et al. (2010) Restoration of impaired intestinal barrier function by the hydrolysed casein diet contributes to the prevention of type 1 diabetes in the diabetes-prone BioBreeding rat. *Diabetologia* 2010;53: 2621–2628
17. Zandecki M, Vanden Berghe P, Depoortere I, Geboes K, Peeters T, et al. Characterization of myenteric neuropathy in the jejunum of spontaneously diabetic BB-rats. *Neurogastroenterol Motil* 2008;20: 818–828
18. Like AA, Biron CA, Weringer EJ, Byman K, Sroczynski E, et al. Prevention of diabetes in BioBreeding/Worcester rats with monoclonal antibodies that recognize T lymphocytes or natural killer cells. *J Exp Med* 1986;164: 1145–1159.
19. Meddings JB, Jarand J, Urbanski SJ, Hardin J, Gall DG. Increased gastrointestinal permeability is an early lesion in the spontaneously diabetic BB rat. *Am J Physiol* 1999;276:G951-7.
20. Neu J, Reverte CM, Mackey AD, Liboni K, Tuhacek-Tenace LM, Hatch M, Li N, Caicedo RA, Schatz DA, Atkinson M. Changes in intestinal morphology and permeability in the biobreeding rat before the onset of type 1 diabetes. *J Pediatr Gastroenterol Nutr* 2005;40:589-595.
21. Vanuytsel T, Vanormelingen C, Vanheel H, Masaoka T, Salim Rasoel S, Tóth J, Houben E, Verbeke K, De Hertogh G, Vanden Berghe P, Tack J, Farré R. From intestinal permeability to dysmotility: the biobreeding rat as a model for functional gastrointestinal disorders. *PLoS One* 2014;29:9(10):e111132.
22. Suzuki H, Mori M, Seto K, Kai A, Kawaguchi C, Suzuki M, Suematsu M Yoneta T, Miura S Ishii H. Helicobacter pylori-associated gastric pro- and antioxidant formation in Mongolian gerbils. Free Radic Biol Med 1999;26:679-684
23. Thomas A, Burant A, Bui N, Graham D, Yuva-Paylor L.A, Paylor R. Marble burying reflects a repetitive and perseverative behavior more than novelty-induced anxiety. *Psychopharmacol (Berl)* 2009;204:361-373
24. Prut L, Belzung C. The open field as a paradigm to measure the effect of drugs on anxiety-like behavior: a review. *Eur J Pharmacol* 2003;403:3-33
25. Walsh RN, Cummins RA. The Open-Field Test: a critical review. *Psychol Bull* 1976;83:482-504.
26. Vanheel H, Vicario M, Vanuytsel T, Van Oudenhove L, Martinez C, Keita ÅV, Pardon N, Santos J, Söderholm JD, Tack J, Farré R. Impaired duodenal mucosal integrity and low-grade inflammation in functional dyspepsia. *Gut* 2014;63:262-271.
27. Piche T, Barbara G, Aubert P, Bruley des Varannes S, Dainese R, Nano JL, Cremon C, Stanghellini V, De Giorgio R, Galmiche JP, Neunlist M. Impaired intestinal barrier integrity in the colon of patients with irritable bowel syndrome: involvement of soluble mediators. *Gut* 2009;58:196-201.

28. Yu O, Ouyang A. Distribution of beta-adrenoceptor subtypes in gastrointestinal tract of nondiabetic and diabetic BB rats. A longitudinal study. Dig Dis Sci. 1997 Jun;42(6):1146-53.
29. Meehan CJ, Fleming S, Smith W, Baird JD. Idiopathic megacolon in the BB rat. *Int J Exp Pathol* 1994;75:37-42.
30. Suzuki H, Miura S, Liu YY, Tsuchiya M, Ishii H. Substance P induces degranulation of mast cells and leukocyte adhesion to venular endothelium. Peptides 1995;16:1447-1452.
31. Camilleri M, Lasch K, Zhou W. Irritable bowel syndrome: methods, mechanisms, and pathophysiology. The confluence of increased permeability, inflammation, and pain in irritable bowel syndrome. *Am J Physiol Gastrointest Liver Physiol* 2012;303:G775-785.
32. Vanuytsel T, van Wanrooy S, Vanheel H, Vanormelingen C, Verschueren S, Houben E, Salim Rasoel S, Tóth J, Holvoet L, Farré R, Van Oudenhove L, Boeckxstaens G, Verbeke K, Tack J. Psychological stress and corticotropin-releasing hormone increase intestinal permeability in humans by a mast cell-dependent mechanism. *Gut* 2014;63:1293-1299.
33. Furuta GT, Nieuwenhuis EE, Karhausen J, Gleich G, Blumberg RS, Lee JJ, Ackerman SJ. Eosinophils alter colonic epithelial barrier function: role for major basic protein. Am J Physiol *Gastrointest Liver Physiol* 2005;289:G890-897.
34. Kristjansson G, Venge P, Wanders A, Loof L, Hallgren R Clinical and subclinical intestinal inflammation assessed by the mucosal patch technique: studies of mucosal neutrophil and eosinophil activation in inflammatory bowel diseases and irritable bowel syndrome. *Gut* 2004;53: 1806–1812.
35. Malle E, Furtmuller PG, Sattler W, Obinger C Myeloperoxidase: a target for new drug development? *Br J Pharmacol* 2007;152: 838–854.
36. Shen L, Weber CR, Raleigh DR, Yu D, Turner JR Tight junction pore and leak pathways: a dynamic duo. *Annu Rev Physiol* 2011;73: 283–309.
37. Tran L, Greenwood-Van Meerveld B. Age-associated remodeling of the intestinal epithelial barrier. *J Gerontol A Biol Sci Med Sci* 2013;68:1045-1056.
38. Mullin JM, Valenzano MC, Verrecchio JJ, Kothari R. Age- and diet-related increase in transepithelial colon permeability of Fischer 344 rats. *Dig Dis Sci* 2002;47:2262-2270.
39. Zihni C, Mills C, Matter K, Balda MS. Tight junctions: from simple barriers to multifunctional molecular gates. *Nat Rev Mol Cell Biol* 2016;17:564-580.
40. Bruewer M, Luegering A, Kucharzik T, et al. Proinflammatory cytokines disrupt epithelial barrier function by apoptosis-independent mechanisms. *Journal of Immunology* 2003;171:6164–6172.
41. Arrieta MC, Madsen K, Doyle J, et al. Reducing small intestinal permeability attenuates colitis in the IL10 gene-deficient mouse. *Gut* 2009;58:41-48
42. Keita AV & Söderholm JD Mucosal permeability and mast cells as targets for functional gastrointestinal disorders *Curr Opin Pharmacol*. 2018;43:66-71

43. Gunter WD, Shepard JD, Foreman RD, Myers DA, Greenwood-van Meerveld B. Evidence for visceral hypersensitivity in high-anxiety rats. *Physiol Behav* 2000;69:379–382
44. Elsenbruch S, Wang L, Hollerbach S, Schedlowski M, Tougas G. Pseudo-affective visceromotor responses and HPA axis activation following colorectal distension in rats with increased cholinergic sensitivity. *Neurogastroenterol Motil* 2004;16:801–809
45. Low-level repeated exposure to diazinon and chlorpyrifos decrease anxiety-like behavior in adult male rats as assessed by marble burying behavior *Neurotoxicology*2015;50:149-156.
46. Neurochemical responses to antidepressants in the prefronta cortex of mice and their efficacy in preclinical models of anxiety-like and depression-like behavior: Psychopharmacology (Berl) 2008;197:567-580.
47. Nébot-Vivinus M, Harkat C, Bzioueche H, Cartier C, Plichon-Dainese R, Moussa L, Eutamene H, Pishvaie D1, Holowacz S, Seyrig C, Piche T, Theodorou V. Multispecies probiotic protects gut barrier function in experimental models. *World J Gastroenterol*. 2014;20(22):6832-43.
48. Sessenwein JL, Baker CC, Pradhananga S, Maitland ME, Petrof EO, Allen-Vercoe E, Noordhof C, Reed DE, Vanner SJ, Lomax AE. Protease-mediated suppression of DRG neuron excitability by commensal bacteria. J Neurosci 2017;37(48):11758-11768.
49. Brugman S, Klatter FA, Visser JTJ, Wildeboer ACM, Harmsen HJM, Rozing J, Bos NA. Antibiotic treatment partially protects against type 1 diabetes in the Bio-Breeding diabetes-prone rat. Is the gut flora involved in the development of type 1 diabetes? *Diabetologia*. 2006;49:2105-2108.
50. Valladares R, Sankar D, Li N, Lai KK, Abdelgeliel AS, Gonzalez CF, Wasserfall CH, Larkin J, Schatz D, Atkinson MA, Triplett EW, Neu J, LorcaGL. Lactubacillus johnsonii N6.2 mitigates the development of type 1 diabetes in BB-DP rats. *Plos one*. 2010;5(5):e10507.

Table 1: Cytokines mRNA expression

	Age	BBDR	BBDP-N	P-value
IFNγ	160	1±0.31	2.71±1.12	ns
	220	1±0.69	2.08±0.69	ns
IL-13	160	1±0.55	33.65±10.04	<0.001
	220	1±0.23	2.49±1.43	ns
IL-1β	160	1±0.20	4.93±1.58	<0.05
	220	1±0.31	0.46±0.29	ns
IL-4	160	1±0.06	10.05±2.46	<0.001
	220	1±0.10	1.12±0.77	ns
iNOS	160	1±0.51	0.63±3.51	ns
	220	1±1.38	12.27±5.60	<0.01
TNF-α	160	1±0.43	0.62±1.11	ns
	220	1±1.99	5.41±2.86	ns

Data are expressed as mean±SEM. ns: not significant

Supplementary table 1: PCR primers

gene	***reverse***	***forward***
Cln-1	CCACTAATGTCGCCAGACCT	ATTGGCATGAAGTGCATGAG
Cln-2	TGGCACCAACATAAGAACTT	GGCTATTAGGCACATCGAT
Occl	ATGTCTGTGAGGCCTTTTGA	TACATGTCATTGCTTGGTGC
ZO-1	CCCTCTgATCATTCCACACA	TTTAGACATGCGCTCTTCCT
IFNγ	TATCTGGAGGAACTGGCAAAAG	TGCGATTCGATGACACTTATGT
IL-13	CCAGTGCGGAGATCCACATC	GGTCCACGCTCCATACCATG
IL-1β	CGTGGAGCTTCCAGGATGAG	CGTCATCATCCCACGAGTCA
IL-4	CAGACGTCCTTACGGCAACA	AGCACGGAGGTACATCACGT
TNFα	GATCGGTCCCAACAAGGAGG	GCTTGGTGGTTTGCTACGAC
iNOS	ACCCAAGGTCTACGTTCAAGACA	CACATCCCGAGCCATGC
HPRT	GCCACATCAACAGGACTCTTGTAG	GCGAAAGTGGAAAAGCCAAGT

Figure legends

Figure 1. Colonic permeability in BBDP-N vs. BBDR rats.

After removal of neuromuscular layers, colonic tissue was mounted in Ussing chambers. Average transepithelial electrical resistance (TEER) between 90 and 120 minutes after mounting was measured using voltage deflections induced by bipolar current pulses of 50 µA with a duration of 200 ms (A). Macromolecular passage through colonic barrier was studied by adding FITC-dextran 4kDa to luminal side and collecting samples into basolateral compartment. Average fluorescence between 90 and 120 minutes after mounting was measured to determine macromolecular permeability (B). Data are expressed as Mean±SEM * $p<0.05$.

Figure 2. Polymorphonuclear cells infiltration.

PMN cells were numbered in the colonic lamina propria following H&E coloration (A). Myeloperoxidase concentration was quantified in mucosal / submucosal layers of BBDP-N and BBDR rats (B). Representative pictures of PMN cells in the lamina propria of 50 and 220 days old rats. Scale bar = 50µm (C). PMN cells were counted in myenteric ganglia following H&E staining (D). Representative pictures of PMN cells in myenteric ganglia of 50 and 220 days old rats. Scale bar = 100µm (E) CM: circular muscle; Cr: Crypt; Ep: Epithelium; LM: Longitudinal muscle; LP: lamina propria; PMN: polymorphonuclear. Data are expressed as Mean±SEM * $p<0.05$; ** $p<0.01$; *** $p<0.001$

Figure 3. Eosinophils contribution to colonic inflammation.

A chromotrope 2R staining was performed to number eosinophils in the lamina propria (A). Eosinophil peroxidase concentration was quantified in mucosal / submucosal layers of BBDP-N and BBDR rats (B).. Representative pictures of eosinophils in the lamina propria of 50 and 220 days old rats. Scale bar = 100µm (C). Data are expressed as Mean±SEM * $p<0.05$; ** $p<0.01$; *** $p<0.001$

Figure 4. Mast cells contribution to colonic inflammation.

Mast cells were numbered in colonic lamina propria by immunohistochemistry in BBDP-N (N) and BBDR rats (A). Representative pictures of mast cells infiltration in the lamina propria of 50 and 220 days old rats. Scale bar = 100µm (B). Data are expressed as Mean±SEM * $p<0.05$; ** $p<0.01$; *** $p<0.001$

Figure 5. Colonic sensitivity and compliance in BBDP-N vs. BBDR rats.

Colonic sensitivity was assessed in 160 (A) and 220 (C) days old rats. A balloon was inflated in rat distal colon from 15 to 60 mmHg with 15 mmHg increments. Each distension was applied twice and lasted 20 seconds with a 4-min interval. Visceromotor response to distension was recorded by a telemetric implant with electrodes attached to the abdominal musculature. For each distension pressure, corresponding volume was recorded in order determine wall tension applied to colonic wall. A linear regression analysis was performed and slopes and intercepts of regression curves were compared between groups using an F-test. Compliance was determined by calculating the volume injected in the rectal probe for each pressure measurement at 160 (B) and 220 days (D). For compliance experiments, data are expressed as Mean±SEM *$p<0.05$; ** $p<0.01$; *** $p<0.001$

Figure 6. Anxiety-like symptoms.

Anxiety-like symptoms assessed in age at different ages (50, 90 and 220 days old) with the open field test evaluating number of squares crossed over the 5 min of recording (A), the number of entries in the inner zone (B) the time spent in the inner zone and the time spent in the inner zone (C) and the marble burying test (D). Representative pictures of the marble burying after 20 min of test (E). Data are expressed as Mean±SEM* $p<0.05$

Figure 7. Correlations between permeability and inflammation.

Positive correlations (Spearman test) were found between lamina proprial passage of FITC-dextran4 kDa and PNM colonic lamina proprial density (A), eosinophil density (B) and mast cells density (C) for all age groups. PMN: poymorphonuclear cells.

Supplementary figure 1: Colonic expression of junction proteins.

Claudin 1 (A), 2 (B), ZO-1 (C) and Occludin (D) gene expression, n=6 per group. Data are expressed as Mean±SEM

Supplementary Figure 2: Correlation with colonic sensitivity.

No correlations were found between the VMR response to the last pressure (60mmHg) and the density of inflammatory cells in the colonic lamina propria eosinophil (A) or mast cells (B) or PMN in the myenteric plexus (C) or the intestinal permeability to Dextran FITC 4kDa (D) for the oldest rat (220 d.o). VMR: visceromotor response, ggl: ganglion.

Figure 1

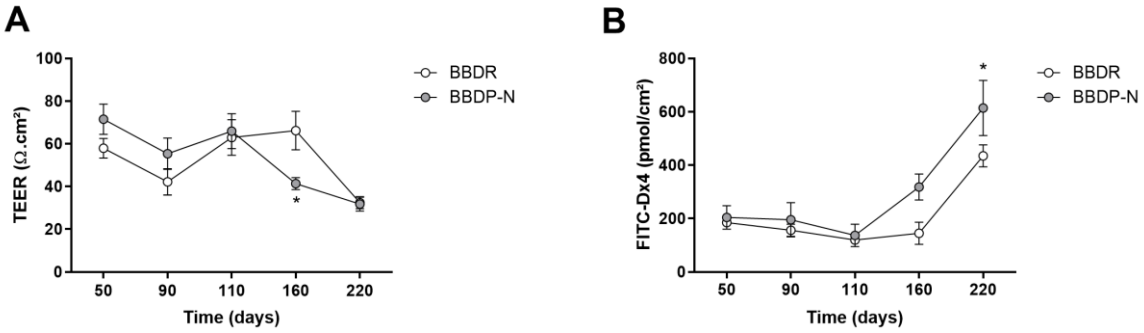
A
TEER (Ω.cm²)
100
80
60
40
20
0
50
90
110
160
220
Time (days)
*
BBDR
BBDP-N
B
FITC-Dx4 (pmol/cm²)
800
600
400
200
0
50
90
110
160
220
Time (days)
*
BBDR
BBDP-N

Figure 2

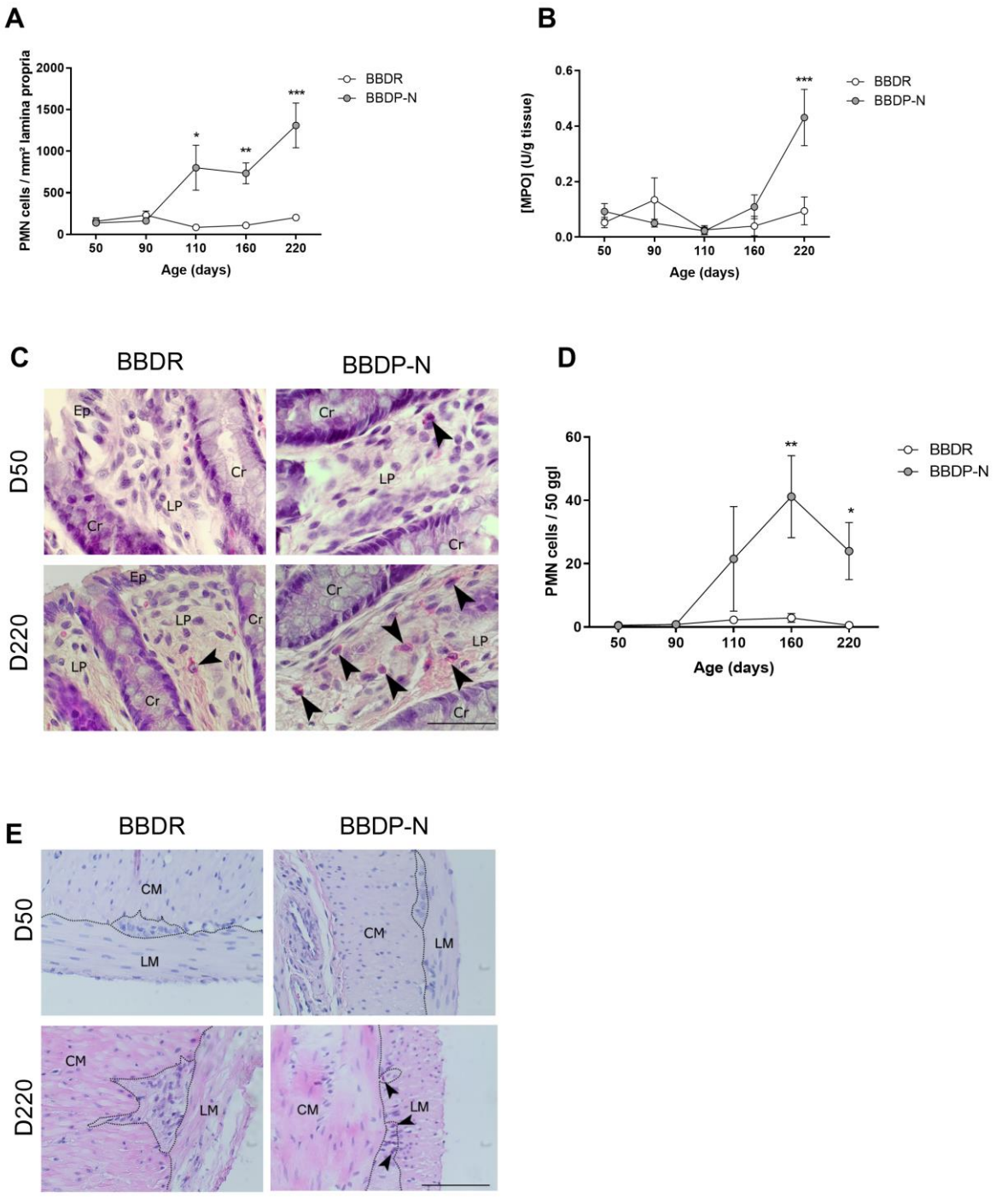
A
PMN cells / mm² lamina propria
2000
1500
1000
500
0
50
90
110
160
220
Age (days)
*
**
***
BBDR
BBDP-N
B
[MPO] (U/g tissue)
0.6
0.4
0.2
0.0
50
90
110
160
220
Age (days)
***
BBDR
BBDP-N
C
BBDR
BBDP-N
D50
D220
Ep
Cr
LP
D
PMN cells / 50 ggl
60
40
20
0
50
90
110
160
220
Age (days)
**
*
BBDR
BBDP-N
E
BBDR
BBDP-N
D50
D220
CM
LM

Figure 3

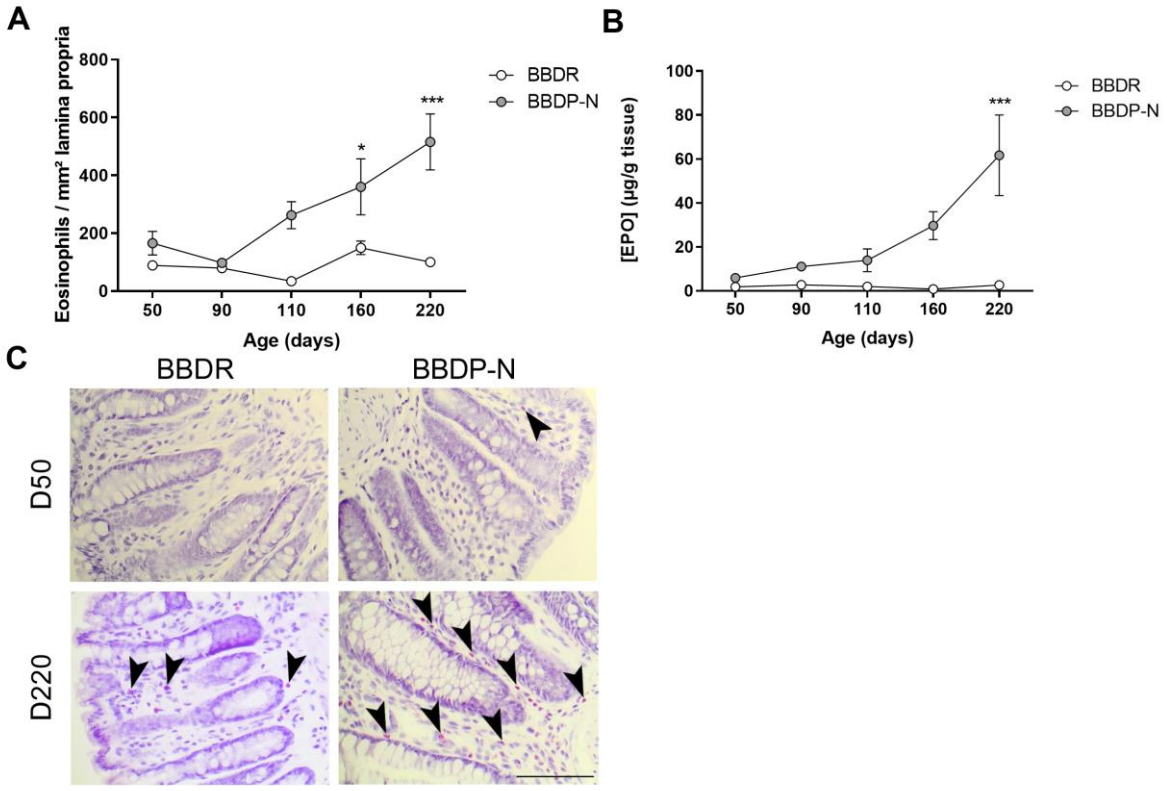
A
Eosinophils / mm² lamina propria
800
600
400
200
0
50
90
110
160
220
Age (days)
*
***
BBDR
BBDP-N
B
[EPO] (µg/g tissue)
100
80
60
40
20
0
50
90
110
160
220
Age (days)
***
BBDR
BBDP-N
C
BBDR
BBDP-N
D50
D220

Figure 4

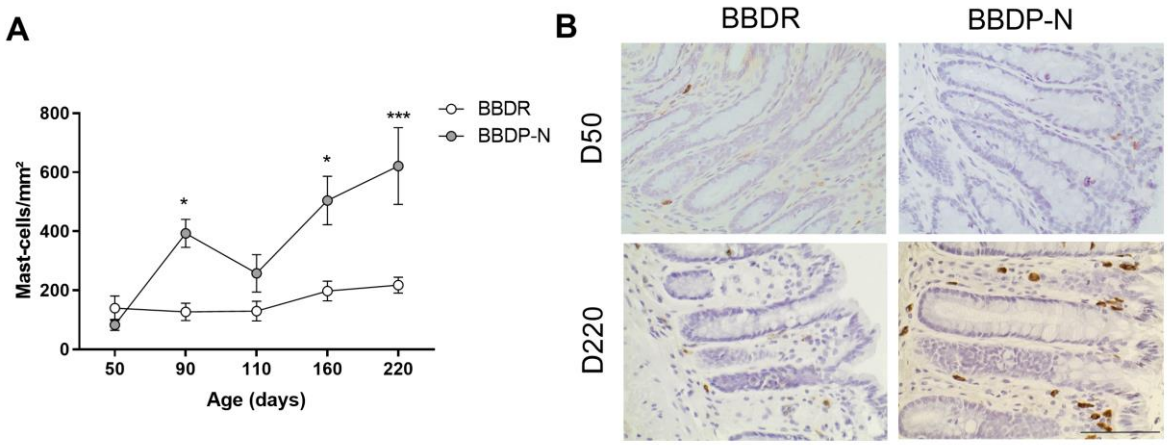
A
800
600
400
200
0
Mast-cells/mm²
50
90
110
160
220
Age (days)
*
*
***
BBDR
BBDP-N
B
BBDR
BBDP-N
D50
D220

Figure 5

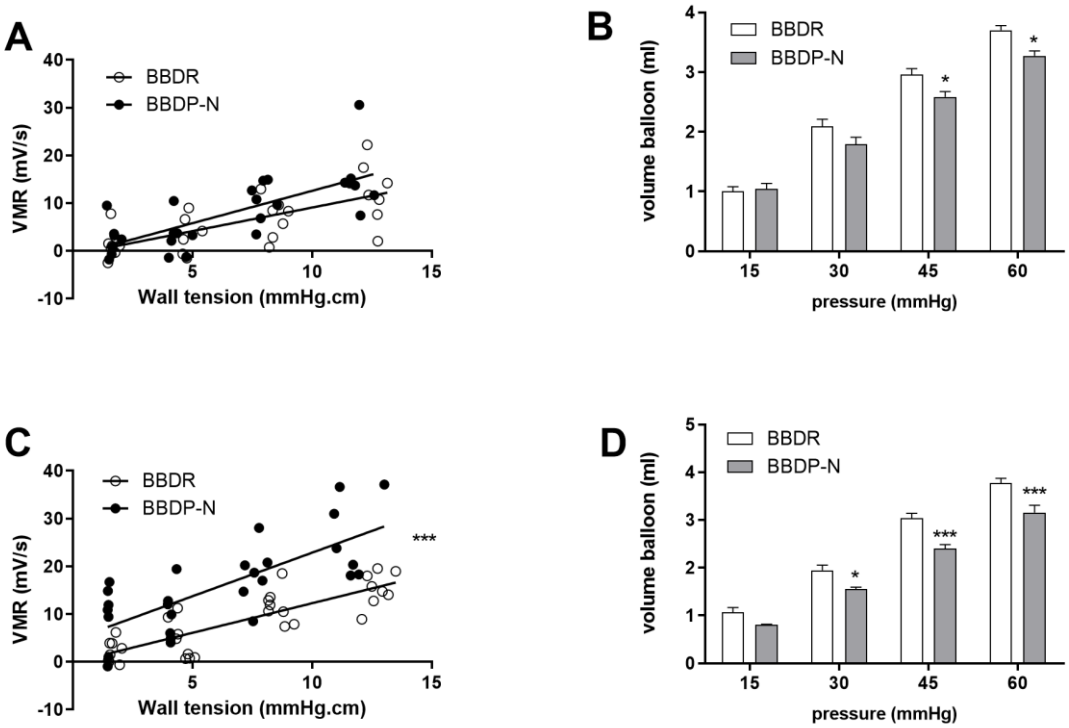
A
BBDR
BBDP-N
VMR (mV/s)
Wall tension (mmHg.cm)
B
BBDR
BBDP-N
volume balloon (ml)
pressure (mmHg)
C
BBDR
BBDP-N
VMR (mV/s)
Wall tension (mmHg.cm)
***
D
BBDR
BBDP-N
volume balloon (ml)
pressure (mmHg)
*
***

Figure 6

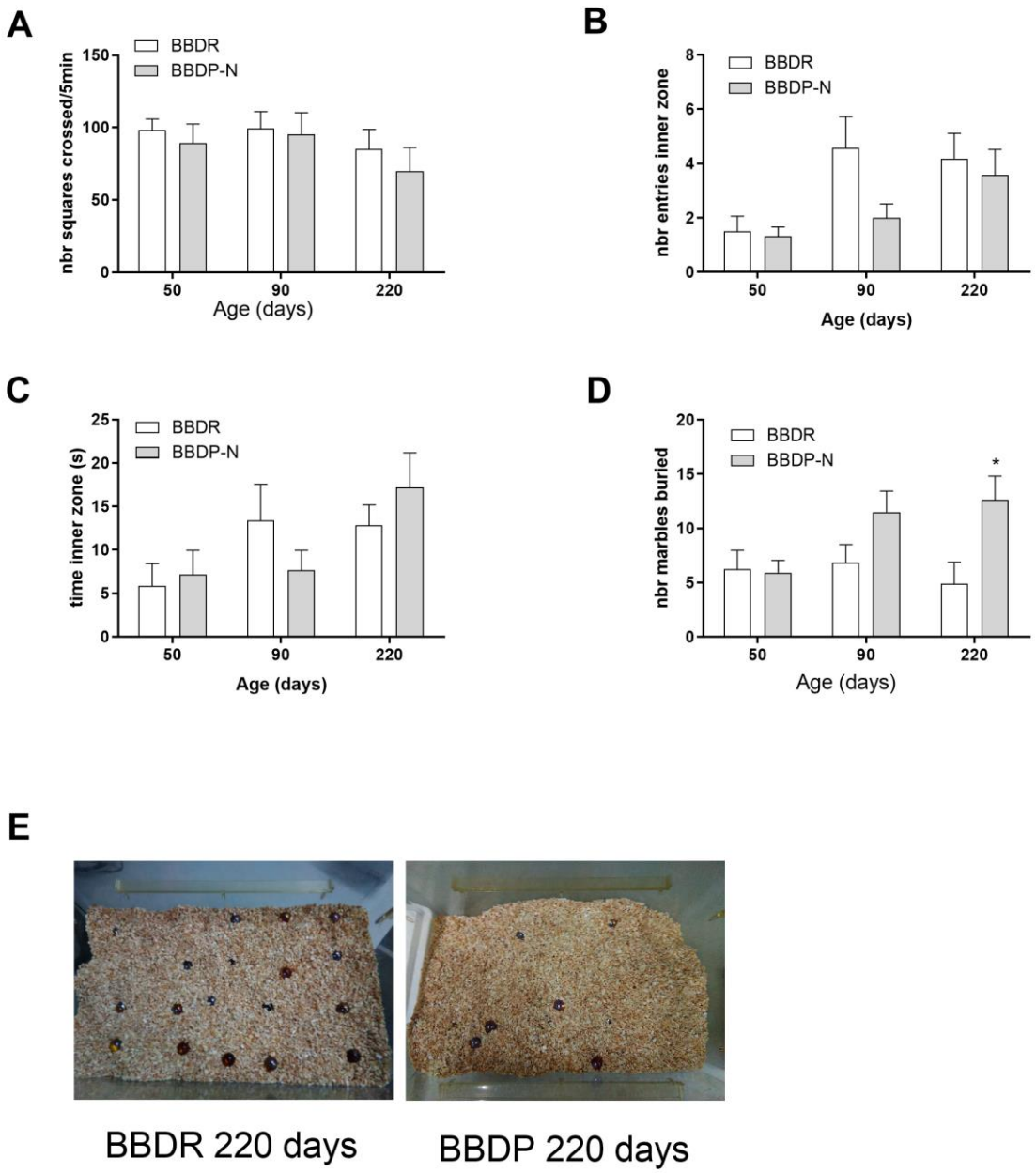
A
BBDR
BBDP-N
nbr squares crossed/5min
150
100
50
0
50
90
220
Age (days)
B
BBDR
BBDP-N
nbr entries inner zone
8
6
4
2
0
50
90
220
Age (days)
C
BBDR
BBDP-N
time inner zone (s)
25
20
15
10
5
0
50
90
220
Age (days)
D
BBDR
BBDP-N
nbr marbles buried
20
15
10
5
0
*
50
90
220
Age (days)
E
BBDR 220 days
BBDP 220 days

Figure 7

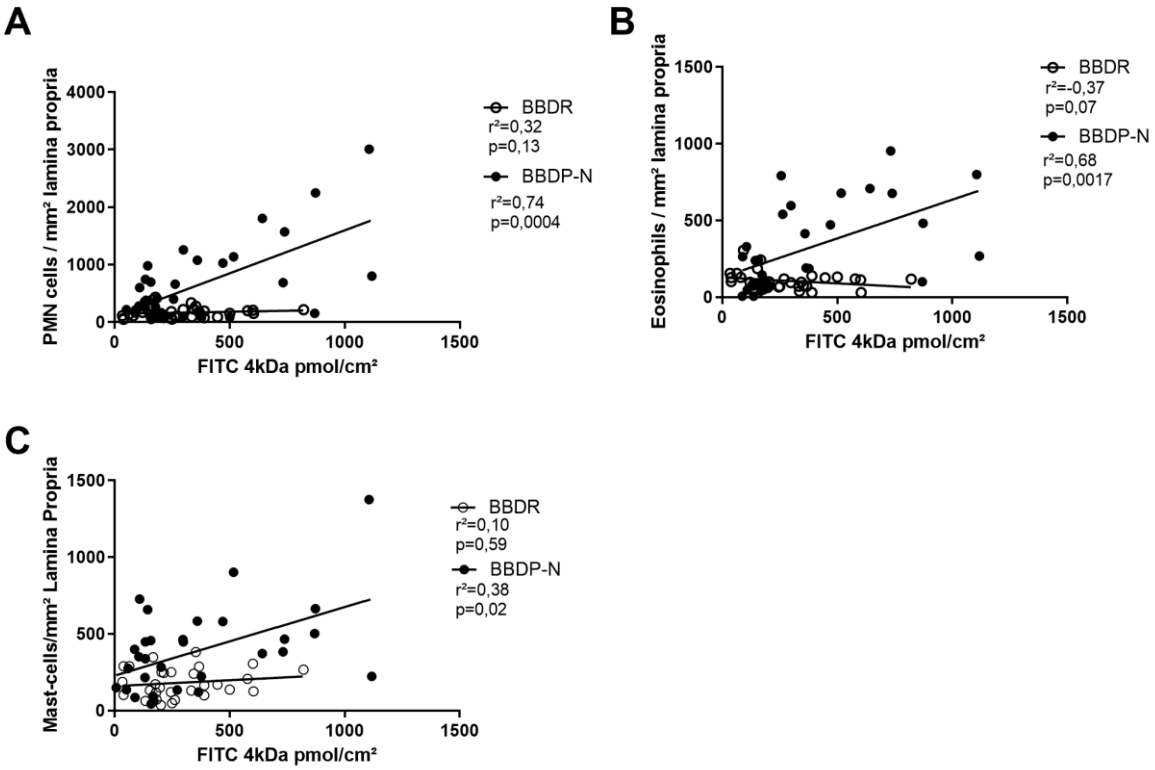
A
PMN cells / mm² lamina propria
4000
3000
2000
1000
0
0
500
1000
1500
FITC 4kDa pmol/cm²
BBDR
r²=0,32
p=0,13
BBDP-N
r²=0,74
p=0,0004
B
Eosinophils / mm² lamina propria
1500
1000
500
0
0
500
1000
1500
FITC 4kDa pmol/cm²
BBDR
r²=-0,37
p=0,07
BBDP-N
r²=0,68
p=0,0017
C
Mast-cells/mm² Lamina Propria
1500
1000
500
0
0
500
1000
1500
FITC 4kDa pmol/cm²
BBDR
r²=0,10
p=0,59
BBDP-N
r²=0,38
p=0,02

Supplementary Figure 1

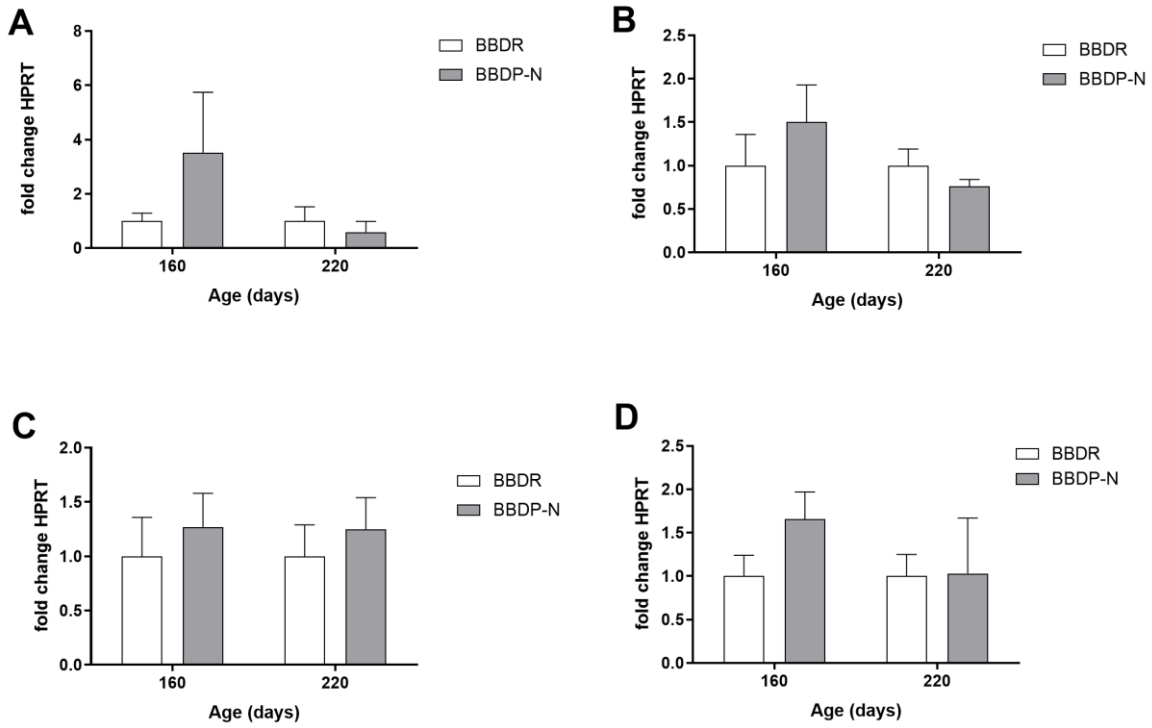

Supplementary Figure 2